

TRENDS IN ULTRACOOL DWARF MAGNETISM. II. THE INVERSE CORRELATION BETWEEN X-RAY ACTIVITY AND ROTATION AS EVIDENCE FOR A BIMODAL DYNAMO

B. A. COOK¹, P. K. G. WILLIAMS², AND E. BERGER²

Draft: January 14, 2021

ABSTRACT

Observations of magnetic activity indicators in solar-type stars exhibit a relationship with rotation with an increase until a “saturation” level and a moderate decrease in activity in the very fastest rotators (“supersaturation”). While X-ray data have suggested that this relationship is strongly violated in ultracool dwarfs (UCDs; spectral type $\gtrsim M7$), the limited number of X-ray detections has prevented firm conclusions. In this paper, we analyze the X-ray activity-rotation relation in 38 ultracool dwarfs. Our sample represents the largest catalog of X-ray active ultracool dwarfs to date, including seven new and four previously-unpublished *Chandra* observations presented in a companion paper. We identify a substantial number of rapidly-rotating UCDs with X-ray activity extending two orders of magnitude below the expected saturation level and measure a “supersaturation”-type anticorrelation between rotation and X-ray activity. The scatter in UCD X-ray activity at a fixed rotation is ~ 3 times larger than that in earlier-type stars. We discuss several mechanisms that have been proposed to explain the data, including centrifugal stripping of the corona, and find them to be inconsistent with the observed trends. Instead, we suggest that an additional parameter correlated with both X-ray activity and rotation is responsible for the observed effects. Building on the results of Zeeman-Doppler imaging of UCD magnetic fields and our companion study of radio/X-ray flux ratios, we argue that this parameter is the magnetic field topology, and that the large scatter in UCD X-ray fluxes reflects the presence of two dynamo modes that produce distinct topologies.

Subject headings: stars: low mass — stars: magnetic fields — stars: rotation — stars: activity

1. INTRODUCTION

Magnetic field generation in the Sun relies on differential rotation in the radiative-convective boundary, and it is therefore expected that this $\alpha\Omega$ dynamo (Parker 1955) will not be responsible for the magnetic fields of stars that are fully convective (dwarfs with spectral types $\gtrsim M3$, or masses $\lesssim 0.35M_{\odot}$; Chabrier & Baraffe 1997). It was thus originally anticipated that magnetic activity would not be found in the “ultracool dwarfs” (UCDs), very-low-mass stars and brown dwarfs with spectral types $\gtrsim M7$ (Kirkpatrick et al. 1999; Martín et al. 1999a). X-ray and H α emission, which generally trace magnetic activity, are indeed significantly suppressed in these objects (Basri & Marcy 1995; Mohanty & Basri 2003; Gizis et al. 2000; Mohanty & Basri 2003; West et al. 2004; Stelzer et al. 2006a; Reiners & Basri 2008; Berger et al. 2010). However, the first detection of radio emission, another tracer of magnetism, from a brown dwarf by Berger et al. (2001) affirmed that UCDs can, in fact, generate significant magnetic fields, and this result has been confirmed by subsequent observations (Berger 2002, 2006; Hallinan et al. 2006; Reiners & Basri 2007; Osten et al. 2009; Berger et al. 2010; Reiners & Basri 2010; Morin et al. 2010; Antonova et al. 2013).

Rotation plays a key role in many stellar dynamo models, including the $\alpha\Omega$ dynamo, and studies of the relationship between rotation and magnetic activity therefore shed light on the dynamo process. Solar-type stars obey

a well-known relationship in which rapid rotation leads to increasing X-ray and H α emission relative to L_{bol} , the stellar bolometric luminosity, up to a “saturation” level. In the X-ray band, the saturation level is $L_X/L_{\text{bol}} \approx 10^{-3}$, and it is reached at rotation periods $P_{\text{rot}} \lesssim 2\text{--}3$ days (e.g., Pizzolato et al. 2003; Wright et al. 2011). These data are generally taken to support a rotationally-powered dynamo with saturation possibly originating in saturation of the dynamo itself (Vilhu & Walter 1987), centrifugal stripping of the corona (Jardine & Unruh 1999), or filling of the entire stellar surface with magnetic active regions (Vilhu 1984). The same overall relationship is observed in early- and mid-M dwarfs (Delfosse et al. 1998; Mohanty & Basri 2003). There is also evidence for a “supersaturation” effect in which the fastest rotators (projected rotational velocity $v \sin i \gtrsim 100 \text{ km s}^{-1}$) have activity levels that are depressed by factors of $\sim 2\text{--}3$ ($L_X/L_{\text{bol}} \approx 10^{-3.5}$; Randich et al. 1996; Stepień et al. 2001; Wright et al. 2011). Supersaturation is not observed in H α (Marsden et al. 2009).

Despite the presumed cessation of the $\alpha\Omega$ dynamo at the transition to full convection, solar-type activity-rotation relations are seen in mid-M dwarfs (Delfosse et al. 1998; Mohanty & Basri 2003). New phenomena begin to appear, however, in the UCD regime. UCDs exhibit an enhanced supersaturation-like effect in X-rays and H α , with L_X/L_{bol} and $L_{\text{H}\alpha}/L_{\text{bol}}$ decreasing by 1–2 orders of magnitude at the highest rotational velocities (James et al. 2000; Berger et al. 2008a; Reiners & Basri 2010). UCD radio emission, on the other hand, *increases* with rotation, with no indications of saturation in even the fastest rotators (McLean et al. 2012). The interpretation of these results is complicated by the number of other changes occurring in this regime, such as the aforemen-

bacook@princeton.edu

¹ Department of Astrophysical Sciences, Princeton University, Princeton, NJ 08544, USA.

² Harvard-Smithsonian Center for Astrophysics, 60 Garden St., Cambridge, MA 02138, USA.

tioned general dropoff of UCD coronal and chromospheric emissions, which is possibly due to decoupling of the increasingly neutral stellar atmospheres from the magnetic fields (Mohanty *et al.* 2002) or more efficient trapping of energetic electrons (Berger *et al.* 2008a, 2010). Furthermore, the fully convective nature of UCDs suggests that a separate dynamo mechanism is in operation, which could quite plausibly have a different dependence on rotation than the $\alpha\Omega$ dynamo (e.g., Durney *et al.* 1993).

In this paper, we build on the observations and database described in Williams *et al.* (2013a, hereafter Paper 1) to investigate the X-ray activity-rotation relation in ultracool dwarfs. We assemble a comprehensive sample of UCDs with both X-ray and rotation measurements, including the new measurements presented in Paper 1. We proceed by reviewing the sample (§2) and our computation of various stellar parameters (§3). We then analyze the rotation-activity relation in the UCD sample and examine correlations between activity and various rotation parameters (§4). We discuss several mechanisms that have been suggested to explain a decline in activity, comparing their predictions to the observed relations in UCDs, and propose that changes in UCD magnetic topology drive the observed anticorrelation between rotation and X-ray activity (§5). Finally, we review our results and suggest future studies that can test our model (§6).

Throughout this work, we use the notation $[x] \equiv \log_{10} x$, with x being measured in cgs units if it is a dimensional quantity, unless its units are specified otherwise.

2. OBSERVATIONAL DATA

In Paper 1 we described observations of seven UCDs using both *Chandra* and the Karl G. Jansky Very Large Array (VLA). These UCDs were chosen to span a narrow spectral type range but a broad range of projected rotational velocities. All seven targets were detected in the X-ray, while only LHS 2397a AB was detected in the radio. These new observations nearly double the number of UCDs with X-ray detections. Paper 1 also describes our analysis of archival *Chandra* observations of four sources, G 208–44 AB (M5.5+M8.5), G 208–45 (M6), LP 349–25 AB (M8+M9), and DENIS-P J025503.3–470049 (L8), all of which have measured rotation velocities. The first three of these are detected while the last is not.

In Paper 1 we also combined our new measurements with a thorough investigation of the literature to build a database of UCDs having both X-ray and radio measurements. We have augmented this database with measurements of $v \sin i$ from the literature. In Tables 1 and 2 we present the compiled data. Some objects having radio measurements but not $v \sin i$ appear in Paper 1 but not in this work; others have $v \sin i$ measurements but no radio data, and appear only in this work.

3. STELLAR ROTATION PROPERTIES

Stellar X-ray activity is commonly analyzed in terms of the ratio of X-ray to bolometric luminosity, thus indicating what fraction of the total radiative energy is emitted in X-rays. We use the term *X-ray activity* to mean the ratio of X-ray luminosity (L_X , in 0.2–2.0 keV band) to the bolometric luminosity (L_{bol}). We calculate bolometric luminosities as described in the Appendix of Paper 1; in short, we use near-IR absolute magnitudes

and bolometric corrections, taking the *J*- and *K*-band corrections of Wilking *et al.* (1999) for M dwarfs and the *K*-band correction of Nakajima *et al.* (2004) for L dwarfs.

Projected rotation periods are derived from $v \sin i$ and stellar radii. We approximate radii using the empirical mass-luminosity relation of Delfosse *et al.* (2000) in conjunction with the theoretically derived mass-radius relation of Baraffe *et al.* (1998). This method is consistent with Reiners & Basri (2010) and McLean *et al.* (2012), who studied the relationship of H α and radio with rotation, respectively. The stellar radii are fairly constant in the UCD regime, and thus any uncertainties in the rotational period are not dominated by the mass-radius relation. However, we note that, due to the confounding inclination parameter, the rotational periods derived from $v \sin i$ are upper limits. X-ray emission is expected to be mostly isotropic, so there should be no inherent correlation between L_X and $\sin i$.

Noyes *et al.* (1984) first suggested that the relation between rotation and magnetic activity may be better analyzed in terms of the Rossby number $\text{Ro} \equiv P_{\text{rot}}/\tau_c$, where τ_c is the convective turnover time. This proposition has been supported by subsequent work (e.g., Pizzolato *et al.* 2003; Wright *et al.* 2011). We calculate τ_c using the method of Kiraga & Stepień (2007) and Reiners & Basri (2010), noting, however, that the physical meaning of this quantity is ill-defined at low masses (e.g., Kim & Demarque 1996):

$$\tau_c(\text{days}) = \begin{cases} 61.7 - 44.7m, & 0.82 \leq m < 1.30 \\ 25, & 0.65 \leq m < 0.82 \\ 86.9 - 94.3m, & 0.10 \leq m < 0.65 \\ 70, & m \leq 0.10 \end{cases} \quad (1)$$

where $m = M_*/M_\odot$. Because τ_c is taken to be constant for spectral types later than $\sim M7$, the Rossby number is therefore essentially equivalent to the rotation period for almost all of our sample of UCDs. The use of Ro is nonetheless still important because it allows comparison across a broad range of spectral types.

We also calculate the corotation radius, the radius at which the centripetal force of corotation with the star is balanced by gravity:

$$\begin{aligned} R_{\text{corot}}/R_* &= \left(\frac{GM_* P_{\text{rot}}^2}{4\pi^2 R_*^3} \right)^{1/3} \\ &\approx 41m^{1/3} \left(\frac{P_{\text{rot}}}{1 \text{ day}} \right)^{2/3} \left(\frac{R_*}{R_J} \right)^{-1}, \end{aligned} \quad (2)$$

with R_J the radius of Jupiter. The ratio of the corotation radius to the stellar radius is often used as a measure of the strength of centrifugal stripping effects in the corona (Jardine & Unruh 1999; James *et al.* 2000).

4. X-RAY ACTIVITY TRENDS

The X-ray activity of our ultracool dwarf sample is plotted against the rotation period, Rossby number, and corotation radius in Figure 1. Also included for comparison are the samples of Pizzolato *et al.* (2003) and James *et al.* (2000), who studied the X-ray activity-rotation relation in A–M6 and M0–M5 dwarfs, respectively. To enhance clarity, we plot the same data excluding known X-ray flares in Figure 2.

Table 1
UCDs with X-ray and $v \sin i$ measurements

2MASS Identifier	Other Name	SpT	J (mag)	K_s (mag)	d (pc)	$[L_{\text{bol}}]$ $[L_{\odot}]$	$v \sin i$ (km s $^{-1}$)	References		
(1)	(2)	(3)	(4)	(5)	(6)	(7)	(8)	(S)	(D)	(V)
08294949+2646348	LHS 248	M6.5	8.23	7.26	3.6	-3.09	11.0 ± 2	1	2	3
¶ 10481258-1120082	LHS 292	M6.5	8.86	7.93	4.5	-3.15	<3	1	4	5
¶ 22285440-1325178	GJ 4281	M6.5	10.77	9.84	11.3	-3.13	7.0 ± 2	6	4	3
11571691+2755489	CTI 115638.4+280000	M7	14.32	13.34	49.1	-3.26	10.5 ± 2	7	8	3
13142039+1320011 AB	NLTT 33370 AB	M7	9.75	8.79	16.4	-2.40	45 ± 5	9	9	10
14563831-2809473	LHS 3003	M7	9.96	8.93	6.4	-3.29	5 ± 2	11	4	5
16553529-0823401	vB 8	M7	9.78	8.82	6.5	-3.21	9.0 ± 2	1	12	3
¶ 11554286-2224586	LP 851-346	M7.5	10.93	9.88	9.7	-3.32	33 ± 3	13	13	5
¶ 15210103+5053230	NLTT 40026	M7.5	12.01	10.92	16.2	-3.30	40 ± 4	11	11	5
¶ 00275592+2219328 AB	LP 349-25 AB	M8	10.61	9.57	13.2	-2.93	56.0 ± 6.0	11	14	15
03205965+1854233	LP 412-31	M8	11.76	10.64	14.5	-3.29	15 ± 4.5	11	16	5
¶ 11214924-1313084 AB	LHS 2397a AB	M8	11.93	10.73	14.3	-3.36	20.0 ± 2	17	4	3
¶ 18432213+4040209	LHS 3406	M8	11.31	10.31	14.1	-3.16	5 ± 3.2	11	4	5
19165762+0509021	vB 10	M8	9.91	8.77	6.1	-3.30	6.5 ± 2	18	18	3
01273917+2805536	CTI 012657.5+280202	M8.5	14.04	12.86	34.8	-3.44	11.0 ± 2	11	11	3
07075327-4900503		M8.5	13.23	12.11	15.1	-3.85	10.0 ± 2	19	4	3
14542923+1606039 Ba	Gl 569 Ba	M8.5	11.14	10.02	9.8	-3.39	19 ± 2	20	21	22
18353790+3259545	LSPM J1835+3259	M8.5	10.27	9.17	5.7	-3.52	44 ± 4	11	16	5
¶ 01095117-0343264	LP 647-13	M9	11.69	10.43	11.1	-3.48	13 ± 2	11	11	5
03393521-3525440	LP 944-20	M9	10.72	9.55	5.0	-3.81	26 ± 3	11	16	5
08533619-0329321	LHS 2065	M9	11.21	9.94	8.5	-3.52	13.5 ± 2	11	4	5
10481463-3956062		M9	9.54	8.45	4.0	-3.54	18 ± 2	5	19	5
11592743-5247188	1RXS J115928.5-524717	M9	11.43	10.32	10.1	-3.48	~25	23	24	24
14284323+3310391	LHS 2924	M9	11.99	10.74	10.8	-3.63	11.0 ± 2	19	4	3
14542923+1606039 Bb	Gl 569 Bb	M9	11.65	10.43	9.8	-3.58	6 ± 3	20	21	22
15010818+2250020	TVLM 513-46546	M9	11.87	10.71	9.9	-3.67	60.0 ± 2	19	4	3
00242463-0158201	BRI B0021-0214	M9.5	11.99	10.54	12.1	-3.49	33 ± 3	25	4	5
00274197+0503417	PC 0025+0447	M9.5	16.19	14.96	72.0	-3.67	13 ± 3	26	26	27
07464256+2000321 AB		L0	11.76	10.47	12.2	-3.36	31 ± 3	28	11	29
06023045+3910592	LSR J0602+3910	L1	12.30	10.87	10.6	-3.67	9 ± 3	30	30	29
13054019-2541059 AB	KelU-1 AB	L2	13.41	11.75	18.7	-3.56	76 ± 8	11	11	29
05233822-1403022		L2.5	13.08	11.64	13.4	-3.82	21 ± 3	11	16	29
00361617+1821104	LSPM J0036+1821	L3.5	12.47	11.06	8.8	-3.99	45 ± 5	31	19	29
14501581+2354424 B	HD 130948 B	L4	13.90	13.30	17.9	-4.28	62 ± 4	32	33	22
14501581+2354424 C	HD 130948 C	L4	14.20	12.60	17.9	-4.00	86 ± 6	32	33	22
12281523-1547342 AB		L5	14.38	12.77	20.2	-3.93	22.0 ± 2	11	11	3
15074769-1627386		L5	12.83	11.31	7.3	-4.23	32 ± 3	31	16	29
¶ 02550357-4700509		L8	13.25	11.56	5.0	-4.58	67 ± 13	11	34	29

References. — Columns are (S), spectral type; (D), distance; and (V), $v \sin i$. [1] Henry et al. (1994), [2] Schmitt & Liefke (2004), [3] Mohanty & Basri (2003), [4] van Altena et al. (1995), [5] Reiners & Basri (2010), [6] Kirkpatrick et al. (1991), [7] Fleming et al. (1993), [8] Kirkpatrick et al. (1995), [9] Lépine et al. (2009), [10] McLean et al. (2011), [11] Cruz et al. (2003), [12] Gliese & Jahreik (1991), [13] Crifo et al. (2005), [14] Gatewood & Coban (2009), [15] Deshpande et al. (2012), [16] Cruz et al. (2007), [17] Freed et al. (2003), [18] Berger et al. (2008b), [19] Reid et al. (2008), [20] Lane et al. (2001), [21] Stelzer (2004), [22] Konopacky et al. (2012), [23] Hambaryan et al. (2004), [24] Robrade & Schmitt (2009), [25] Reid et al. (1995), [26] McLean et al. (2012), [27] Martín et al. (1999b), [28] Berger et al. (2009), [29] Reiners & Basri (2008), [30] Berger et al. (2010), [31] Berger et al. (2005), [32] Stelzer et al. (2006a), [33] Potter et al. (2002), [34] Costa et al. (2006)

Note. — Rows marked with a pilcrow (¶) indicate sources with new measurements presented in Paper I. Col. (3) is spectral type. Cols. (4) and (5) 2MASS (Skrutskie et al. 2006).

Figure 1 clearly shows the pre-saturation and saturation regimes in stars earlier than type M6.5. UCDs are systematically faster rotators than earlier-type stars in terms of both period and Rossby number, having $P_{\text{rot}} < 2$ day and $\text{Ro} < 0.03$. The UCDs do not follow the rotation-activity trend seen in earlier-type stars, which would predict that their X-ray emission should be saturated near $L_X/L_{\text{bol}} \approx 10^{-3}$. Instead, 22 of the 38 sources show X-ray emission at $L_X/L_{\text{bol}} \leq 10^{-4}$ and five have $L_X/L_{\text{bol}} \leq 10^{-5}$. This dropoff is much stronger than that associated with supersaturation in solar-type stars, in which L_X/L_{bol} drops only to $\sim 10^{-3.5}$ (Wright et al. 2011). All L dwarfs (with the exception of one shallow non-detection) have activity levels well below the saturation value.

The dropoff in UCD X-ray activity appears to be cor-

related with rotation. We convey this effect in a simple way in Figure 3, which plots the fraction of UCDs with $L_X/L_{\text{bol}} > 10^{-4}$ when binned in terms of $v \sin i$. Flaring measurements and upper limits less constraining than $L_X/L_{\text{bol}} > 10^{-3}$ are not included in this analysis. There is a lack of relatively X-ray bright UCDs at $v \sin i \gtrsim 20$ –30 km s $^{-1}$. Interestingly, McLean et al. (2012) found that a large fraction of UCDs above this cutoff are relatively radio-bright. In Paper I we argued that these two effects are related.

Another effect seen in Figures 1 and 2 is that the overall scatter in X-ray activity among rapid rotators is larger in UCDs than in solar-type stars. For solar-type stars in the Pizzolato et al. (2003) sample with $P_{\text{rot}} < 1$ d, the standard deviation in activity is $\sigma([L_X/L_{\text{bol}}]) = 0.25$, while for UCDs in the same rotation range, $\sigma([L_X/L_{\text{bol}}]) =$

Table 2
X-ray data for UCDs with $v \sin i$ measurements

2MASS Identifier	SpT	$[L_{\text{bol}}]$ [L_{\odot}]	St.	X-Ray Band (keV)	$[L_X]$ [erg s^{-1}]	$[L_X/L_{\text{bol}}]$	Ref.
(1)	(2)	(3)	(4)	(5)	(6)	(7)	(8)
08294949+2646348	M6.5	-3.09	-	0.1-2.4	26.5	-4.0	1
10481258-1120082	M6.5	-3.15	-	0.2-2.0	25.7	-4.7	*
22285440-1325178	M6.5	-3.13	-	0.2-2.0	25.7	-4.8	*
11571691+2755489	M7	-3.26	-	0.1-2.4	< 28.3	< -2.0	4
13142039+1320011	AB M7	-2.40	Q	0.2-2.0	27.6	-3.6	5
			F	0.2-2.0	28.3	-2.9	5
14563831-2809473	M7	-3.29	-	0.1-2.4	26.2	-4.1	7
16553529-0823401	M7	-3.21	Q	0.1-2.4	26.9	-3.5	8
			F	0.1-2.4	27.5	-2.9	7
11554286-2224586	M7.5	-3.32	Q	0.2-2.0	25.9	-4.4	*
			F	0.2-2.0	26.8	-3.5	*
15210103+5053230	M7.5	-3.30	-	0.2-2.0	25.7	-4.6	*
00275592+2219328	AB M8	-2.93	Q	0.2-2.0	25.8	-4.8	*
			F	0.2-2.0	26.3	-4.3	*
03205965+1854233	M8	-3.29	Q	0.3-8.0	27.2	-3.1	10
			F	0.3-8.0	29.7	-0.6	10
11214924-1313084	AB M8	-3.36	-	0.2-2.0	27.1	-3.1	*
18432213+4040209	M8	-3.16	Q	0.2-2.0	26.5	-4.0	*
			F	0.2-2.0	27.1	-3.3	*
19165762+0509021	M8	-3.30	Q	0.2-2.0	25.2	-5.1	11
			F	0.2-2.0	25.7	-4.6	11
01273917+2805536	M8.5	-3.44	-	0.1-2.4	< 27.8	< -2.3	4
07075327-4900503	M8.5	-3.85	-	0.1-2.4	< 27.4	< -2.3	4
14542923+1606039	Ba M8.5	-3.39	-	0.5-8.0	26.9	-3.3	12
18353790+3259545	M8.5	-3.52	-	0.2-2.0	< 24.5	< -5.6	11
01095117-0343264	M9	-3.48	Q	0.2-2.0	25.2	-4.9	*
			F	0.2-2.0	26.1	-4.0	*
03393521-3525440	M9	-3.81	Q	0.1-10.0	< 24.0	< -5.7	14
			F	0.1-10.0	25.6	-4.2	14
08533619-0329321	M9	-3.52	Q	0.3-0.8	26.5	-3.6	15
			F	0.1-2.4	27.6	-2.5	16
10481463-3956062	M9	-3.54	-	0.2-2.0	25.1	-4.9	17
11592743-5247188	M9	-3.48	Q	0.1-2.4	< 27.9	< -2.2	18
			F	0.1-2.4	28.8	-1.3	18
14284323+3310391	M9	-3.63	-	0.1-2.4	< 25.5	< -4.4	4
14542923+1606039	Bb M9	-3.58	-	0.5-8.0	26.9	-3.1	12
15010818+2250020	M9	-3.67	Q	0.3-2.0	24.9	-5.0	20
			F	0.3-2.0	27.3	-2.6	20
00242463-0158201	M9.5	-3.49	-	0.2-2.0	< 25.1	< -4.9	21
00274197+0503417	M9.5	-3.67	-	0.3-8.0	< 26.2	< -3.7	17
07464256+2000321	AB L0	-3.36	-	0.2-2.0	< 25.2	< -5.0	23
06023045+3910592	L1	-3.67	-	0.2-2.0	< 25.0	< -4.9	21
13054019-2541059	AB L2	-3.56	-	0.1-10.0	25.3	-4.7	25
05233822-1403022	L2.5	-3.82	-	0.2-2.0	< 25.2	< -4.5	21
00361617+1821104	L3.5	-3.99	-	0.2-8.0	< 24.9	< -4.7	26
14501581+2354424	B L4	-4.28	-	0.5-8.0	< 25.7	< -3.6	12
14501581+2354424	C L4	-4.00	-	0.5-8.0	< 25.7	< -3.9	12
12281523-1547342	AB L5	-3.93	-	0.3-8.0	< 26.6	< -3.0	17
15074769-1627386	L5	-4.23	-	0.2-8.0	< 24.8	< -4.6	26
02550357-4700509	L8	-4.58	-	0.2-2.0	< 24.3	< -4.7	*

References. — Col. (8) is the X-ray luminosity reference. [*]: Paper 1, [1] Delfosse *et al.* (1998), [2] Mohanty & Basri (2003), [3] Reiners & Basri (2010), [4] Fleming *et al.* (1993), [5] Williams *et al.* (2013b, in preparation), [6] McLean *et al.* (2011), [7] Schmitt *et al.* (1995), [8] Güdel *et al.* (1993), [9] Deshpande *et al.* (2012), [10] Stelzer *et al.* (2006b), [11] Berger *et al.* (2008b), [12] Stelzer *et al.* (2006a), [13] Konopacky *et al.* (2012), [14] Rutledge *et al.* (2000), [15] Robrade & Schmitt (2008), [16] Schmitt & Liefke (2002), [17] Stelzer *et al.* (2012), [18] Hambaryan *et al.* (2004), [19] Robrade & Schmitt (2009), [20] Berger *et al.* (2008a), [21] Berger *et al.* (2010), [22] Martín *et al.* (1999b), [23] Berger *et al.* (2009), [24] Reiners & Basri (2008), [25] Audard *et al.* (2007), [26] Berger *et al.* (2005)

Note. — Col. (4) is the state of the source: quiescent (Q), flaring (F), or indeterminate/unknown (-). L_X has been normalized to the 0.2-2 keV bandpass as described in the text.

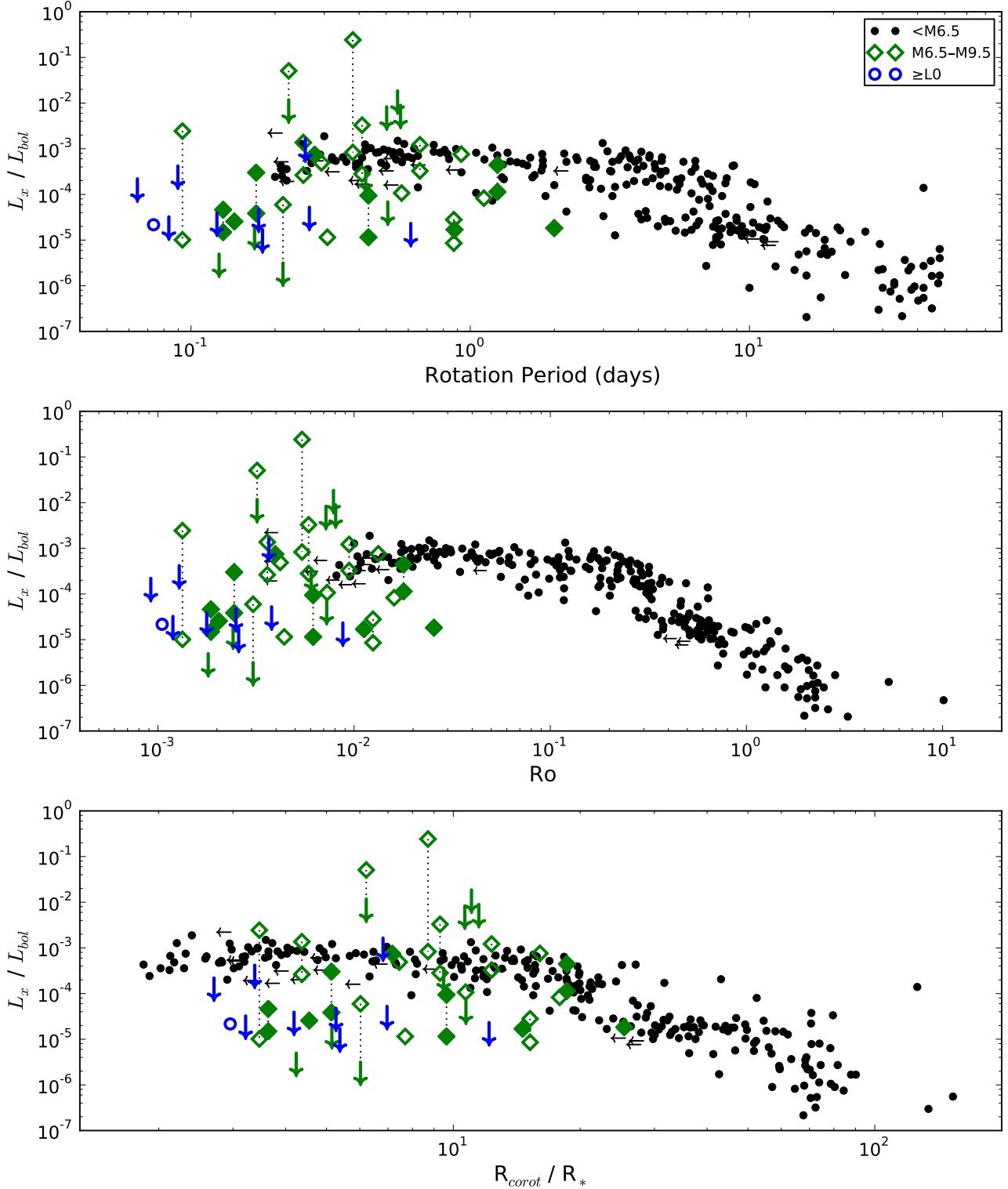


Figure 1. X-ray activity versus various stellar rotation parameters, as calculated in §3. The parameters are rotation period (*upper panel*), Rossby number (*middle panel*), and the centrifugal stripping parameter (Jardine & Unruh 1999, *lower panel*). The UCD rotation parameters are formally upper limits due to the unknown inclination. Plotted are objects from this work, James et al. (2000), and Pizzolato et al. (2003). Points connected by a dotted line represent quiescent and flaring observations of the same object. Spectral types are denoted by black circles (<M6.5), green diamonds (M6.5–M9.5), and blue circles (\geq L0). Downward-facing arrows indicate X-ray nondetections. Solid colored symbols indicate new measurements presented in Paper I. The <M6.5 outlier at $P_{\text{rot}} \sim 40$ d and $L_X/L_{\text{bol}} \sim 10^{-4}$ is Proxima Centauri, an unusually slowly-rotating M6 dwarf. In non-UCDs, a standard activity-rotation relation with saturation around $L_X/L_{\text{bol}} \approx 10^{-3}$ is seen regardless of the rotation parameter used. UCDs show rapid rotation but activity well below the saturation level. The fastest-rotating UCDs have larger centrifugal stripping parameters than many of the slower-rotating solar-type stars, suggesting that this effect is not responsible for “supersaturation” in UCDs (§5.1).

0.85. This effect is most pronounced when rotation is parametrized in terms of Ro , which has less scatter in the pre-saturation regime than P_{rot} or R_{corot}/R_* .

4.1. Isolating the Role of Rotation

It is important to understand whether the decrease in UCD X-ray activity is caused by faster rotation or is due to trends in other stellar parameters such as temperature, mass, or age. To this end we analyze the relationship between X-ray activity and rotation in a subsample of UCDs in the narrow spectral type range M6.5–M9.5. This subsample removes the influence of effective temperature on activity, as T_{eff} decreases by only ~ 500 K between M6.5 and M9.5 (Luhman *et al.* 2003).

We analyze only nonflaring emission and remove known tight binaries from the sample, consistent with the analysis of Pizzolato *et al.* (2003). Konopacky *et al.* (2012) showed that, in some UCD binaries, $v \sin i$ can differ significantly (by up to 30 km s^{-1}) between components, and it cannot be determined from available data alone whether X-ray activity or rotational velocity are influenced by a blending of the components.

In main-sequence low-mass stars, mass and rotation are correlated (Irwin & Bouvier 2008). However, as shown in Figure 4, $v \sin i$ is not strongly correlated with spectral type within our subsample. Furthermore, the new observations presented in Paper I contribute to the subsample at a wide range of $v \sin i$, so our dataset is capable of isolating the role of rotation despite its restriction to a narrow range of T_{eff} .

We perform regressions to investigate correlations between the various rotational parameters and X-ray activity. Several UCDs in our sample (particularly L dwarfs) are not detected in X-rays, requiring the use of survival analysis methods (e.g., Feigelson & Babu 2012). Our regressions use a maximum likelihood estimator (MLE) method based upon an accelerated failure-time model (method `cenmle`) in the package NADA (Helsel 2005) in the R language. One benefit of this method is that it allows for automatic calculation of the likelihood ratio of the parametrized model to a model without dependence on rotation, yielding a statistical p -value that indicates the strength of the correlation. To estimate the uncertainty in the fit parameters, we performed a bootstrap analysis, running 10,000 iterations on the fit, sampling with replacements and calculating the MLE fit parameters for each sample. The distributions of fit parameters for all regressions are approximately normal, so the standard deviation of the distribution is adopted as the uncertainty of each fit parameter.

The results of the survival analysis regressions are shown in Table 3. Although there is significant scatter in the data, each regression finds that X-ray activity decreases with faster rotation in UCDs. The p -values of the regressions range between $p < 0.02$ and $p < 0.07$. Figure 5 shows the regressions of L_X/L_{bol} against $v \sin i$ derived for both the entire UCD sample and the subsample of M6.5–M9.5 dwarfs. In this and all other cases, the regressions in both the full sample and the rotation-isolating subsample are statistically indistinguishable, which is consistent with a scenario in which there is no correlation between T_{eff} and L_X/L_{bol} within the UCD regime. However, it is clear that T_{eff} strongly affects L_X/L_{bol} in the sense that UCDs behave very differently than *earlier-type objects*

Table 3
X-ray Activity-Rotation Regression Parameters

X	Y	a	b	Prob.
Full UCD sample				
$v \sin i$ (km s^{-1})	L_X	-1.3 ± 0.5	27.0 ± 0.6	$p < 0.02$
$v \sin i$ (km s^{-1})	L_X/L_{bol}	-0.9 ± 0.4	-3.5 ± 0.5	$p < 0.04$
P_{rot} (days)	L_X/L_{bol}	1.0 ± 0.4	-4.1 ± 0.3	$p < 0.02$
Ro	L_X/L_{bol}	1.0 ± 0.4	-2.2 ± 0.9	$p < 0.02$
Subsample: M6.5–M9.5 dwarfs, no binaries				
$v \sin i$ (km s^{-1})	L_X	-1.3 ± 0.6	27.2 ± 0.6	$p < 0.03$
$v \sin i$ (km s^{-1})	L_X/L_{bol}	-1.0 ± 0.6	-3.4 ± 0.6	$p < 0.07$
P_{rot} (days)	L_X/L_{bol}	1.0 ± 0.6	-4.1 ± 0.3	$p < 0.06$
Ro	L_X/L_{bol}	1.0 ± 0.6	-2.3 ± 1.2	$p < 0.06$

Note. — Regression parameters of $[Y] = a[X] + b$, derived using the MLE method described in §4. While significant scatter exists in the data, the likelihood analysis allows us to dismiss no correlation with rotation with reasonable confidence. P -values are calculated from χ^2 values derived by the regression algorithm. Interestingly, the fit for the entire UCD sample is consistent with the subsample of M6.5–M9.5. This indicates that, while later spectral types are systematically faster rotators, spectral type variations alone are not entirely responsible for the observed correlation; rotation has a significant influence on X-ray emission.

with comparable levels of rotation: the mean level of their X-ray activity is significantly lower ($L_X/L_{\text{bol}} \approx 10^{-4.5}$ versus 10^{-3}), there is significantly more scatter in L_X/L_{bol} within the population ($\sigma([L_X/L_{\text{bol}}]) \sim 0.9$ versus 0.3), and there is an anticorrelation between L_X/L_{bol} and rotation as opposed to a null correlation.

5. POSSIBLE CAUSES OF DECREASED X-RAY EMISSION IN UCDS

Our analysis in §4 found evidence for an anticorrelation between X-ray activity and rotation in UCDs, in both in the total UCD sample and in a subsample of M6.5–M9.5 stars, where rotation is not strongly correlated with spectral type and temperature changes by less than $\sim 20\%$. We believe this to be the strongest evidence to date of a breakdown in the standard X-ray activity-rotation relation in UCDs. We now consider possible explanations for this reduction in X-ray activity in UCDs, which we group into two broad categories: explanations that argue for a “supersaturation” mechanism with a causal relation between rapid rotation and reduced activity levels; and “anticorrelations” in which an additional parameter independently affects both rotation and activity, leading to the observed trend.

5.1. Supersaturation Mechanisms

Several explanations for supersaturation of magnetic activity in ultra-fast rotators have been proposed previously, motivated by the mild drop in L_X (factors of ~ 2 – 3) seen in the most rapidly-rotating solar-type (G/K) stars. In these stars the rotationally-driven $\alpha\Omega$ dynamo is believed to generate magnetic activity, and it has been suggested that supersaturation may be due to negative feedback in the dynamo at extremely fast rotation rates (Kitchatinov *et al.* 1994). The $\alpha\Omega$ dynamo is not believed to operate in fully-convective UCDs, and a turbulent dynamo is expected to have only a mild dependence on rotation

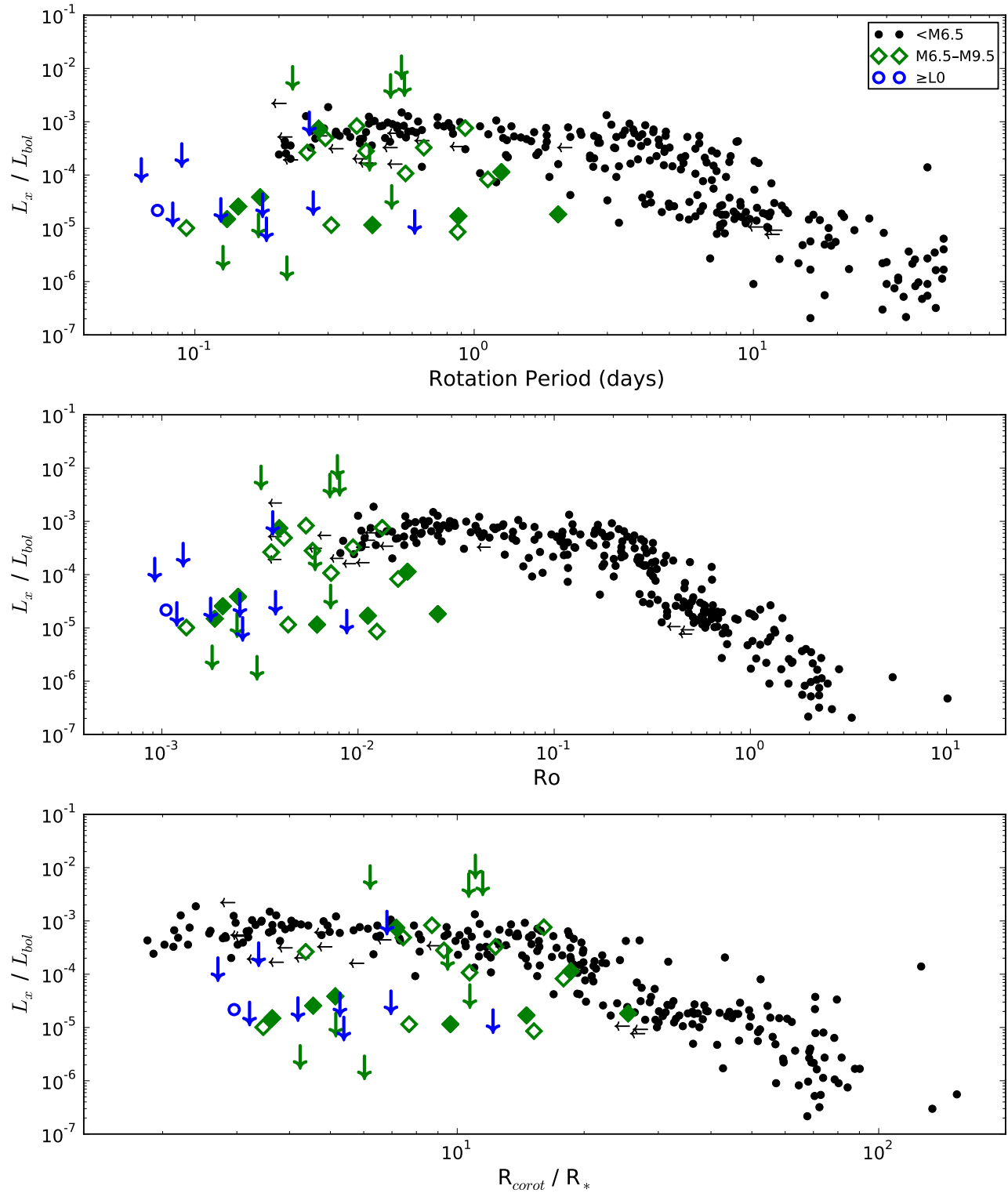


Figure 2. The same as Figure 1, but excluding known X-ray flares.

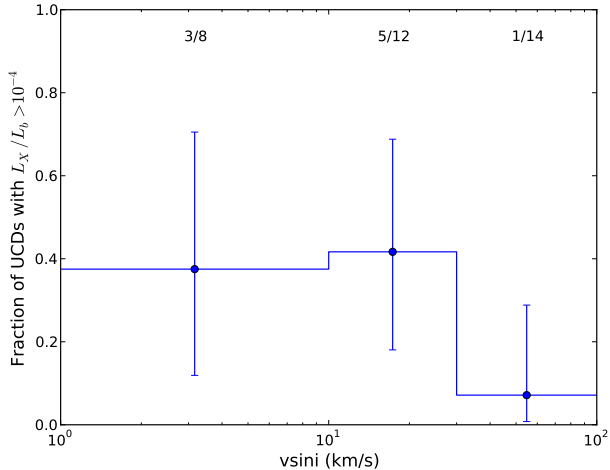


Figure 3. Fraction of UCDs with $L_X/L_{\text{bol}} > 10^{-4}$ as a function of $v \sin i$. Flares and upper limits less constraining than $L_X/L_{\text{bol}} < 10^{-3}$ are not included in the analysis. The fractions above each bin give the actual counts. Error bars are 95% confidence intervals for the binomial distribution computed using an equal-tailed Jeffreys interval.

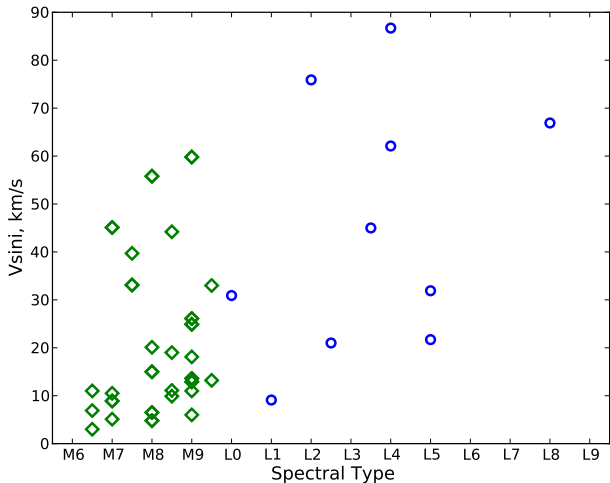


Figure 4. Projected rotational velocity in the UCD sample as a function of spectral type. Blue symbols represent L dwarfs and green symbols represent M dwarfs. L dwarfs are systematically faster rotators. However no strong correlation with spectral type exists over the narrow spectral type regime M6.5–M9.5. Our analysis thus incorporates a subsample of UCDs in this range, in order to isolate the influence of spectral type (temperature) from purely rotational dependences.

(Durney *et al.* 1993). A rotationally-dependent α^2 dynamo, on the other hand, might show supersaturation effects at high rotation, possibly explaining the decrease in coronal emission found here in UCDs. However, radio emission in some UCDs does not saturate or supersaturate with fast rotation (Berger *et al.* 2010; McLean *et al.* 2012), as coronal and chromospheric activity appear to. Instead, radio activity in stars as late as L4 increases with rotation to several orders of magnitude above the saturation level of solar-type stars, implying continued, robust operation of a magnetic dynamo.

Another proposed cause of supersaturation is centrifugal stripping of the coronal envelope (Jardine & Unruh 1999; James *et al.* 2000; Jardine 2004). This model suggests that centrifugal forces in the outer coronae of rapidly

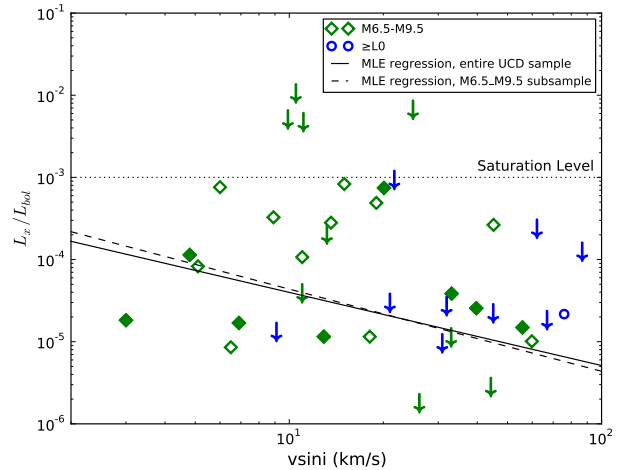


Figure 5. The UCD activity-rotation relation in terms of $v \sin i$. X-ray activity is converted to the 0.2–2.0 keV band (see Paper 1). Symbols and colors are the same as in Figure 1. The solid line shows the MLE regression ($p < 0.07$) for the M6.5–M9.5 subsample that isolates the effects of rotation from those of the large mass and temperature changes that occur across the full UCD sample. The dashed line shows the regression across the full sample ($p < 0.04$), which is statistically indistinguishable.

rotating stars lead to an increase in coronal pressure and density, increasing the X-ray emissions coming from a given coronal volume. The volume of the emitting coronal regions will, however, be limited by the corotation radius. Jardine & Unruh (1999) argue that, in the moderate-rotation regime, the two effects will cancel, leading to X-ray saturation. However, at sufficiently rapid rotation periods the coronal stripping will reduce the overall X-ray emission, causing a supersaturation effect.

The point at which centrifugal stripping would result in supersaturation depends on the characteristic height of magnetic field loops in the corona. Wright *et al.* (2011) claim to find evidence for supersaturation (activity decrease from $L_X/L_{\text{bol}} \approx 10^{-3}$ to $\sim 10^{-3.5}$) in solar-type stars only at values of $R_{\text{corot}}/R_* \approx 2$ –3. Yet, as shown in Figure 1, UCDs with suppressed X-ray emission in our sample have values of R_{corot}/R_* even higher than 10, in the same range as solar-type stars which show saturated emission. If centrifugal stripping is responsible for supersaturation in UCDs, the relative sizes of their coronal loops must be $\gtrsim 5$ times larger than even early M dwarfs. Furthermore, the magnitude of the observed X-ray activity decrease (nearly two orders of magnitude) is much larger than that observed in solar-type stars. We therefore do not find it plausible that centrifugal stripping is the chief mechanism behind the UCDs supersaturation effect.

5.2. Sources of Anticorrelation

The anticorrelation between activity and rotation does not imply a causal connection between the two parameters. Although our analysis indicates a general trend towards lower activity with faster rotation, the existence of pairs of stars with similar spectral types and rotation velocities yet vastly different X-ray activity levels challenges a causal supersaturation interpretation. For example, the M9 dwarfs LHS 2065 and 2MASS J10481463-3956062 ($v \sin i = 13.5$ and 18 km s^{-1} , respectively) likely have similar masses, temperatures, and rotational ve-

locities, yet differ by a factor of ~ 30 in X-ray activity ($[L_X/L_{\text{bol}}] = -3.55$ and -4.95). Indeed, the overall scatter in X-ray activity among rapid rotators is much larger in UCDs than in solar-type stars. We speculate that an additional parameter, weakly correlated with both rotation and activity, is responsible for this large scatter and leads to the observed anticorrelation.

One possible parameter is the effective temperature T_{eff} . The overall decrease in the X-ray emission of UCDs has been attributed to declining values of T_{eff} , via increasingly neutral photospheres that couple to the magnetic field progressively less effectively (Mohanty et al. 2002). However, it is difficult to understand how such a mechanism alone could explain the rotational dependence of X-ray activity found in the current sample of active UCDs, which is observed even in the M6.5–M9.5 subsample that isolates a population of similar temperatures and masses. Purely temperature-dependent arguments additionally cannot explain the widely varying X-ray activity among stars with similar spectral types. We therefore do not consider T_{eff} as the relevant parameter.

Recent spectropolarimetry results suggest that the topology of stellar magnetic fields changes significantly in the fully-convective regime. These results come from the use of Zeeman-Doppler imaging (ZDI) techniques (Semel 1989), which measure Zeeman splitting in the Stokes V line profiles and are thus sensitive to the net magnetic flux over a resolution element (denoted B_V), rather than the total field strength (B_I). Morin et al. (2008) used ZDI to map the large-scale magnetic fields of six fully-convective M3–M4.5 stars, finding in all cases a strong mean field, $\langle B_V \rangle$, in a low-multipolar configuration. Continuing this analysis into the spectral type range M5–M8 (including G 208–45, VB 8, and VB 10 from our sample), Morin et al. (2010) found that late-M stars exhibit either strong large-scale magnetic fields (similar to mid-M stars) or fields with weak large-scale components, dominated by small-scale fields (similar to solar-type stars). A key result was that both topologies were observed in stars with similar masses and rotation periods. Numerical modeling suggests that two separate dynamo regimes, producing magnetic fields with differing topologies, could be mutually stable in low-mass stars, leading to the observed bimodality in magnetic field structure (Morin et al. 2011; Gastine et al. 2013). McLean et al. (2012) argued for the existence of a similar bimodality based on radio observations.

Figure 6 shows that the large-scale magnetic field strengths for the objects studied in Morin et al. (2010) correlate with rotation and spectral type in a remarkably similar fashion to the observed X-ray activity/rotation/spectral-type relations in M dwarfs. Mid-M dwarfs (mostly rapid rotators with $\text{Ro} < 0.1$) have “saturated” large-scale field strengths (~ 600 G) independent of rotation. Late-M dwarfs ($\text{Ro} \lesssim 10^{-2}$) show large scatter in their large-scale strengths, with some occupying the saturated branch and others falling as much as an order of magnitude below the saturated level. This is strongly reminiscent of the behavior seen in the measurements of L_X/L_{bol} presented in this work.

In Paper I, we suggested that the topology of the magnetic field affects radio and X-ray luminosity ratios, with large-scale fields being associated with relatively high

X-ray activity levels. The trends in X-ray activity and rotation that we describe here are consistent with this proposal. In this scenario, the large scatter in X-ray activity as a function of rotation is due to the varying strength of the large-scale stellar field components. Differences in the X-ray emission from stars with similar rotational velocities and spectral types (such as LHS 2065 and 2MASS J10481463-3956062) may trace the relative topology of their magnetic fields.

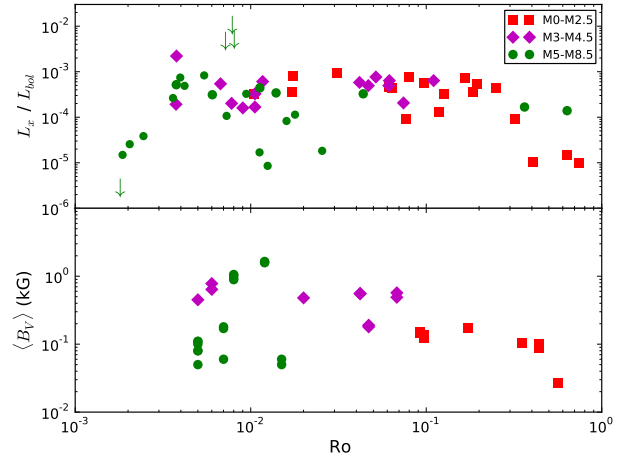


Figure 6. Similarity in the Rossby-number dependence of L_X/L_{bol} and $\langle B_V \rangle$. *Upper panel:* reproduction of the nonflaring data points from the middle panel of Figure 1, with a slightly altered color coding. *Lower panel:* reproduction of the ZDI data reported by Donati et al. (2008) and Morin et al. (2008); Morin et al. (2010). Although only three sources overlap between the samples (see text), both panels show similar trends: negative correlation in early-M dwarfs (red), flat relationship in mid-M dwarfs (magenta), and scattered, positive correlation in late-M dwarfs (green).

The physical basis for such a connection is not fully obvious, because well-ordered, large-scale fields might be expected to be less likely to generate the reconnection events that are thought to ultimately power coronal X-ray emission. We suggested in Paper I that the objects with small-scale fields may generate many small reconnection events that are insufficiently energetic to produce X-ray emission in the standard chromospheric evaporation model. We also emphasize that ZDI measurements are sensitive to only some aspects of the full complexity of stellar magnetic fields. In particular, unresolved oppositely-directed field components — such as the footpoints of compact coronal loops — cancel out in ZDI data, and observations of FeH molecular lines suggest that ZDI measurements are sensitive to $\lesssim 15\%$ of the total magnetic field (Reiners & Basri 2009). A more detailed physical treatment must handle such “blind spots” carefully.

The anticorrelation between rotation and X-ray activity will be enhanced if stars with large-scale fields also exhibit generally slower rotational velocities. Although Gastine et al. (2013) found that large-and-small scale topologies can be generated in the same rotation regime, stellar rotational evolution may depend on the large-scale magnetic topologies. Spin-down processes may be affected by the increased moment of inertia from an extended corona, and magnetic braking is believed to be more significant in large-scale fields than in tangled, high-multipolar fields (Reiners & Mohanty 2012). We speculate that stars with

large-scale, dipolar fields may form with similar rotation values as low-activity, multipolar stars but spin down more quickly, reinforcing the observed anticorrelation between activity and rotation.

Little overlap exists between UCDs observed in X-ray and those with measured magnetic topologies. [Morin et al. \(2010\)](#) find that [GJ 1245 B](#) and [VB 10](#) ($L_X/L_{\text{bol}} = -4.3$ and -5.1 in quiescence) show no evidence of strong large-scale components, consistent with our interpretation. [VB 8](#) is also found to be dominated by small-scale fields, although it shows higher quiescent activity ($L_X/L_{\text{bol}} = -3.5$). [McLean et al. \(2011\)](#) suggest that observed periodicities in radio emission in [NLTT 33370 AB](#) ($L_X/L_{\text{bol}} = -3.6$ in quiescence) suggest the existence of significant large-scale field components, although this has not been confirmed with ZDI observations. Further study is required to examine the connection between magnetic topology and coronal activity measurements in UCDs, although this is complicated by the difficulty of obtaining ZDI measurements of rapidly-rotating stars.

6. SUMMARY AND CONCLUSIONS

We present the most complete sample to date of ultracool dwarfs ($\gtrsim M7$) with measured rotational velocities and X-ray luminosities. Included in this sample are new measurements from [Paper 1](#). Combining these with data available from the literature, our sample contains 38 objects later than M6. All of these UCDs are fast rotators ($P_{\text{rot}} \lesssim 1$ day) yet the majority show X-ray luminosity at least an order of magnitude lower than predicted from their bolometric luminosities and the established saturated activity-rotation relation for early-M dwarfs.

We find evidence for an anticorrelation between X-ray activity and rotation in the UCD sample that is much more extreme than the supersaturation effects observed in rapidly-rotating solar-type stars, suggesting that UCDs do not merely represent the rapidly-rotating end of the same activity-rotation relation found in solar-type stars. This conclusion is reinforced by the much larger scatter in X-ray activity levels found in UCDs compared to earlier-type stars.

As radio activity was found by [McLean et al. \(2012\)](#) to increase with faster rotation even in the UCD regime, it is unlikely that the decrease in X-ray activity is due to a decrease in the effectiveness of the magnetic dynamo. Centrifugal stripping alone is also unlikely to be responsible, as the supersaturated UCDs would require extremely large coronae for centrifugal effects to be significant. The overall scatter in quiescent activity between stars with similar spectral types and rotational velocities suggests that a separate parameter, correlated weakly with both rotation and X-ray activity, is required to match the observed trends.

We suggest that the magnetic field topology represents such a parameter, as large-scale field strengths in convective stars correlate with rotation and spectral type in a remarkably similar fashion to X-ray activity. Ultracool Dwarfs with large-scale fields may spin down more efficiently than those with weaker, tangled fields, enhancing the observed anticorrelation.

This framework can be related to the observed correlations between radio and X-ray emission in UCDs. As discussed in [Paper 1](#), there is evidence that UCDs can be divided into two groups: objects that are radio-bright

and X-ray-faint, and those that are radio-faint but X-ray-bright. In our proposed scenario, the former would harbor weak tangled fields, while the latter would harbor stronger, dipolar fields. The bimodality observed in the latest-type objects implies that rapid rotators can be radio-faint and X-ray bright, but that slow rotators ($\text{Ro} \gtrsim 0.1$) are not expected to reach the extremely high radio/X-ray flux ratios ($\sim 10^4$ above expectations) seen in some UCDs.

Further observations are required to increase the number of UCDs with known magnetic topologies and X-ray fluxes, but we speculate that X-ray activity should be correlated with the large-scale fraction of the magnetic fields. Further ZDI measurements (performed in conjunction with X-ray observations) can help illuminate the effect of large-scale topology on coronal emissions. Obtaining an improved understanding of the radio properties of the fastest rotators should also be a high priority. The newly upgraded Karl G. Jansky Very Large Array, with its sensitivity increase of nearly an order of magnitude compared to the original system, offers an excellent opportunity to improve on previous work. In addition, theoretical models should continue to push into extremely-rapid rotation regimes, to provide accurate explanations for the trends being found observationally.

B. A. C. thanks Jonathan McDowell and Marie Machacek for their advice and comments on drafts of this work. This work is supported in part by the National Science Foundation REU and Department of Defense ASSURE programs under NSF Grant no. 1262851 and by the Smithsonian Institution. E. B. and P. K. G. W. acknowledge support for this work from the National Science Foundation through Grant AST-1008361, and from the National Aeronautics and Space Administration through Chandra Award Number GO2-13007A issued by the Chandra X-ray Observatory Center, which is operated by the Smithsonian Astrophysical Observatory for and on behalf of the National Aeronautics Space Administration under contract NAS8-03060. This research has made use of the SIMBAD database, operated at CDS, Strasbourg, France, and NASA's Astrophysics Data System.

REFERENCES

- Antonova, A., Hallinan, G., Doyle, J. G., et al. 2013, *A&A*, 549, A131
- Audard, M., Osten, R. A., Brown, A., et al. 2007, *A&A*, 471, L63
- Baraffe, I., Chabrier, G., Allard, F., & Hauschildt, P. 1998, *A&A*, 337, 403
- Basri, G., & Marcy, G. W. 1995, *AJ*, 109, 762
- Berger, E. 2002, *ApJ*, 572, 503
- Berger, E. 2006, *ApJ*, 648, 629
- Berger, E., Ball, S., Becker, K. M., et al. 2001, *Nature*, 410, 338
- Berger, E., Rutledge, R. E., Reid, I. N., et al. 2005, *ApJ*, 627, 960
- Berger, E., Gizis, J. E., Giampapa, M. S., et al. 2008a, *ApJ*, 673, 1080
- Berger, E., Basri, G., Gizis, J. E., et al. 2008b, *ApJ*, 676, 1307
- Berger, E., Rutledge, R. E., Phan-Bao, N., et al. 2009, *ApJ*, 695, 310
- Berger, E., Basri, G., Fleming, T. A., et al. 2010, *ApJ*, 709, 332
- Chabrier, G., & Baraffe, I. 1997, *A&A*, 327, 1039
- Costa, E., Méndez, R., Jao, W. C., et al. 2006, *AJ*, 132, 1234
- Crifo, F., Phan-Bao, N., Delfosse, X., et al. 2005, *A&A*, 441, 653
- Cruz, K., Reid, N., Liebert, J., Kirkpatrick, D., & Lowrance, P. 2003, *AJ*, 126, 2421
- Cruz, K., Reid, N., Kirkpatrick, D., et al. 2007, *AJ*, 133, 439

- Delfosse, X., Forveille, T., Perrier, C., & Mayor, M. 1998, *A&A*, **331**, 581
- Delfosse, X., Forveille, T., Ségransan, D., et al. 2000, *A&A*, **364**, 217
- Deshpande, R., Martín, E. L., Montgomery, M. M., et al. 2012, *AJ*, **144**, 99
- Donati, J. F., Morin, J., Petit, P., et al. 2008, *MNRAS*, **390**, 545
- Durney, B. R., Young, D. S., & Roxburgh, I. W. 1993, *Solar Physics*, **145**, 207
- Feigelson, E. D., & Babu, G. J. 2012, *Modern Statistical Methods for Astronomy* (Cambridge University Press)
- Fleming, T. A., Giampapa, M. S., Schmitt, J. H. M. M., & Bookbinder, J. A. 1993, *ApJ*, **410**, 387
- Freed, M., Close, L., & Siegler, N. 2003, *ApJ*, **584**, 453
- Gastine, T., Morin, J., Duarte, L., et al. 2013, *A&A*, **549**, L5
- Gatewood, G., & Coban, L. 2009, *AJ*, **137**, 402
- Gizis, J., Monet, D., Reid, N., et al. 2000, *AJ*, **120**, 1085
- Gliese, W., & Jahreik, H. 1991, *Preliminary Version of the Third Catalogue of Nearby Stars* (Heidelberg: Astron. Rechen-Institut)
- Güdel, M., Schmitt, J. H. M. M., Bookbinder, J. A., & Fleming, T. A. 1993, *ApJ*, **415**, 236
- Hallinan, G., Antonova, A., Doyle, J. G., et al. 2006, *ApJ*, **653**, 690
- Hambaryan, V., Staude, A., Schwöpe, A. D., et al. 2004, *A&A*, **415**, 265
- Helsel, D. R. 2005, *Nondetects and data analysis: statistics for censored environmental data* (Wiley-Interscience)
- Henry, T. J., Kirkpatrick, J. D., & Simons, D. A. 1994, *AJ*, **108**, 1437
- Irwin, J., & Bouvier, J. 2008, *Proc. IAU*, **4**, 363
- James, D. J., Jardine, M. M., Jeffries, R. D., et al. 2000, *MNRAS*, **318**, 1217
- Jardine, M. 2004, *A&A*, **414**, L5
- Jardine, M., & Unruh, Y. C. 1999, *A&A*, **346**, 883
- Kim, Y. C., & Demarque, P. 1996, *ApJ*, **457**, 340
- Kiraga, M., & Stepień, K. 2007, *Acta Astronomica*, **57**, 149
- Kirkpatrick, D., Reid, N., Liebert, J., et al. 1999, *ApJ*, **519**, 802
- Kirkpatrick, J. D., Henry, T. J., & McCarthy, D. W. 1991, *ApJS*, **77**, 417
- Kirkpatrick, J. D., Henry, T. J., & Simons, D. A. 1995, *AJ*, **109**, 797
- Kitchatinov, L. L., Rüdiger, G., & Küker, M. 1994, *A&A*, **292**, 125
- Konopacky, Q. M., Ghez, A. M., Fabrycky, D. C., et al. 2012, *ApJ*, **750**, 79
- Lane, B. F., Zapatero Osorio, M. R., Britton, M. C., Martín, E. L., & Kulkarni, S. R. 2001, *ApJ*, **560**, 390
- Lépine, S., Thorstensen, J., Shara, M., & Rich, M. 2009, *AJ*, **137**, 4109
- Luhman, K. L., Stauffer, J. R., Muench, A. A., et al. 2003, *ApJ*, **593**, 1093
- Marsden, S. C., Carter, B. D., & Donati, J. F. 2009, *MNRAS*, **399**, 888
- Martín, E., Delfosse, X., Basri, G., et al. 1999a, *AJ*, **118**, 2466
- Martín, E. L., Basri, G., & Zapatero Osorio, M. R. 1999b, *AJ*, **118**, 1005
- McLean, M., Berger, E., Irwin, J., Forbrich, J., & Reiners, A. 2011, *ApJ*, **741**, 27
- McLean, M., Berger, E., & Reiners, A. 2012, *ApJ*, **746**, 23
- Mohanty, S., & Basri, G. 2003, *ApJ*, **583**, 451
- Mohanty, S., Basri, G., Shu, F., Allard, F., & Chabrier, G. 2002, *ApJ*, **571**, 469
- Morin, J., Donati, J. F., Petit, P., et al. 2010, *MNRAS*, **407**, 2269
- Morin, J., Dormy, E., Schrunner, M., & Donati, J.-F. 2011, *MNRAS Lett.*, **418**, L133
- Morin, J., Donati, J.-F., Petit, P., et al. 2008, *MNRAS*, **390**, 567
- Nakajima, T., Tsuji, T., & Yanagisawa, K. 2004, *ApJ*, **607**, 499
- Noyes, R. W., Hartmann, L. W., Baliunas, S. L., Duncan, D. K., & Vaughan, A. H. 1984, *ApJ*, **279**, 763
- Osten, R. A., Phan-Bao, N., Hawley, S. L., Reid, I. N., & Ojha, R. 2009, *ApJ*, **700**, 1750
- Parker, E. N. 1955, *ApJ*, **122**, 293
- Pizzolato, N., Maggio, A., Micela, G., Sciortino, S., & Ventura, P. 2003, *A&A*, **397**, 147
- Potter, D., Martín, E. L., Cushing, M. C., et al. 2002, *ApJL*, **567**, L133
- Randich, S., Schmitt, J. H. M. M., Prosser, C. F., & Stauffer, J. R. 1996, *A&A*, **305**, 785
- Reid, N., Cruz, K., Kirkpatrick, D., et al. 2008, *AJ*, **136**, 1290
- Reid, N., Hawley, S., & Gizis, J. 1995, *AJ*, **110**, 1838
- Reiners, A., & Basri, G. 2007, *ApJ*, **656**, 1121
- . 2008, *ApJ*, **684**, 1390
- . 2009, *A&A*, **496**, 787
- . 2010, *ApJ*, **710**, 924
- Reiners, A., & Mohanty, S. 2012, *ApJ*, **746**, 43
- Robrade, J., & Schmitt, J. H. M. M. 2008, *A&A*, **487**, 1139
- . 2009, *A&A*, **496**, 229
- Rutledge, R. E., Basri, G., Martín, E. L., & Bildsten, L. 2000, *ApJL*, **538**, L141
- Schmitt, J., Fleming, T., & Giampapa, M. 1995, *ApJ*, **450**, 392
- Schmitt, J. H. M. M., & Liefke, C. 2002, *A&A*, **382**, L9
- . 2004, *A&A*, **417**, 651
- Semel, M. 1989, *A&A*, **225**, 456
- Skrutskie, M. F., Cutri, R. M., Stiening, R., et al. 2006, *AJ*, **131**, 1163
- Stelzer, B. 2004, *ApJL*, **615**, L153
- Stelzer, B., Micela, G., Flaccomio, E., Neuhäuser, R., & Jayawardhana, R. 2006a, *A&A*, **448**, 293
- Stelzer, B., Schmitt, J. H. M. M., Micela, G., & Liefke, C. 2006b, *A&A*, **460**, L35
- Stelzer, B., Alcalá, J., Biazzo, K., et al. 2012, *A&A*, **537**, A94
- Stepień, K., Schmitt, J. H. M. M., & Voges, W. 2001, *A&A*, **370**, 157
- van Altena, W. F., Lee, J. T., & Hoffleit, E. D. 1995, *The general catalogue of trigonometric parallaxes* (New Haven: Yale University Observatory)
- Vilhu, O. 1984, *A&A*, **133**, 117
- Vilhu, O., & Walter, F. M. 1987, *ApJ*, **321**, 958
- West, A. A., Hawley, S. L., Walkowicz, L. M., et al. 2004, *AJ*, **128**, 426
- Wilking, B. A., Greene, T. P., & Meyer, M. R. 1999, *AJ*, **117**, 469
- Williams, P. K. G., Cook, B. A., & Berger, E. 2013a, paired paper 1
- Williams, P. K. G., et al. 2013b, in preparation
- Wright, N. J., Drake, J. J., Mamajek, E. E., & Henry, G. W. 2011, *ApJ*, **743**, 48